의학박사학위논문

Alterations in PD-L1 expression associated with acquisition of resistance to ALK inhibitors in *Anaplastic lymphoma kinase*-rearranged lung cancer

Anaplastic lymphoma kinase 유전자가 재배열된 폐암에서 ALK 억제제에 대한 내성 획득과 연관된 PD-L1 발현의 변화

2017 년 2 월

서울대학교 대학원

의학과 분자종양의학 전공

김 수 정

Anaplastic lymphoma kinase 유전자가 재배열된 폐암에서 ALK 억제제에 대한 내성 획득과 연관된 PD-L1 발현의 변화

지도교수: 김 동 완

이 논문을 의학박사학위논문으로 제출함

2016 년 10 월

서울대학교 대학원

의학과 분자종양의학 전공

김 수 정

김수정의 박사학위논문을 인준함

2017 년 1월

위 원 장 _____ (인)

부 위 원 장 _____ (인)

위 원 _____ (인)

위 원 _____ (인)

위 원 _____ (인)

Alterations in PD-L1 expression associated with acquisition of resistance to ALK inhibitors in *Anaplastic lymphoma kinase*-rearranged lung cancer

by Su-Jung Kim, M.D.

(Directed by Professor Dong-Wan Kim, M.D., PhD)

A Thesis Submitted to the Department of Molecular Tumor Biology with Partial Fulfillment of the Requirements for the Degree of Doctor of Philosophy in The Department of Molecular Tumor Biology, Seoul National University College of Medicine

January 2017

Approved by Thesis Committee:

Professor _____Chairman

Professor _____Vice chairman

Professor _____

Professor _____

Professor _____

ABSTRACT

Introduction: Anaplastic lymphoma kinase (ALK) inhibitor is a standard therapy for patients with ALK-rearranged non-small cell lung cancer (NSCLC). However, most patients who respond initially develop resistance over time. Programmed cell death–ligand 1 (PD-L1) expressed on tumor cells induces immune escape and promotes tumor progression. The relationships between the resistance of ALK-positive NSCLC tumors to ALK inhibitors and the programmed cell death-1 (PD-1)/PD-L1 pathway have not been well-defined. Thus, we evaluated alterations in PD-L1 following acquisition of resistance to ALK inhibitors in ALK-positive lung cancer tissues and cell lines.

Materials and Methods: Tumors were analyzed from 26 ALK-positive metastatic NSCLC patients (11 ALK inhibitor-naïve and 15 ALK inhibitor-resistant patients). The expression of PD-L1 and lymphocyte markers were assessed by immunohistochemistry and compared between the tumor specimens before and after treatment with ALK inhibitors. The PD-L1 H-score was calculated as a product of the intensity score (0, no staining; 1, weak staining; 2, moderate staining; and 3, strong staining) and proportion, and PD-L1 positivity was determined by the intensity and proportion using a cutoff of 10%.

We also established ALK inhibitor-resistant cell lines (H3122CR1, LR1, and CH1) by exposing the parental H3122 ALK-translocated lung cancer cell line to ALK inhibitors. Then, the double-resistant cell lines H3122CR1LR1 and CR1CH1 were developed by exposing the crizotinib-resistant cell line H3122CR1 to other

ALK inhibitors. We compared the alterations in PD-L1 expression levels using western blotting, flow cytometry, and quantitative polymerase chain reaction. We also investigated gene expression in H3122, CR1, LR1, CH1, CR1LR1, and CR1CH1 cell lines using RNA sequencing. We examined these properties in single- and double-resistant cell lines, each compared with H3122 parental cell lines. We then examined the associated biological processes and pathways using the differentially expressed gene data.

Results: The mean value of the PD-L1 H-score was 6.5 pre-treatment (ALK inhibitor-naïve cells) and 35.0 post-treatment (ALK inhibitor-resistant cells), and the fold difference was 5.42 (p=0.163). PD-L1 positivity is more evident in post-treatment samples than in pre-treatment samples (3 [20.0%] vs. 0 [0.0%] patients, p=0.175). The mean value of CD68/mm^2 was 181.6±115.4 and 90.8±48.9 in pre-treatment and post-treatment tumor samples, respectively (p=0.030).

In the *in vitro* experiments, PD-L1 was expressed at higher levels in ALK inhibitor-resistant cell lines than in the ALK inhibitor-naïve parental cell line H3122. Furthermore, PD-L1 expression in the double-resistant cell lines was much higher than that in the single resistant cell lines. This trend was consistent at the total protein, surface protein, and mRNA levels.

RNA sequencing demonstrated that expression of immune-related genes, including PGLYRRP4, CCL20, DEFB4A, LTB, and CDH6, was largely different in the single- and double-resistant cells compared with the parental H3122 cells.

The more the cell lines acquired resistance to ALK inhibitors, the higher PD-L1expression was observed. In the analysis of biologic processes and pathways, immune-related pathways, including cytokine pathways, were found to be significantly involved in ALK inhibitor resistance.

Conclusions: PD-L1 expression increased following acquisition of ALK inhibitor resistance in ALK-positive NSCLC patient tumors and cell lines. Interestingly, this trend became more evident as the cells acquired additional resistance. The role of PD/1PD-L1 pathway in ALK inhibitor resistance therefore merits further investigation.

Keywords: anaplastic lymphoma kinase (ALK), lung cancer, ALK inhibitor, resistance, programmed cell death–ligand 1 (PD-L1), immune checkpoint
Student Number: 2011-31138

CONTENTS

LIST OF TABLES AND FIGURES

INTRODUCTION

Lung cancer is the most common cause of cancer mortality worldwide,[1,2] and non-small cell lung cancer (NSCLC) accounts for about 85% of all lung cancers.[3] Oncogenic fusion genes that activate the tyrosine kinase anaplastic lymphoma kinase (ALK) have been identified as oncogenic drivers of NSCLC in 4 to 15% of NSCLC patients.[4,5] Treatment with an ALK tyrosine kinase inhibitor is a standard therapy for patients with ALK-rearranged NSCLC; however, most patients relapse within 1 to 2 years due to the development of drug resistance.[6] In contrast to epidermal growth factor receptor (EGFR)-mutant NSCLC in which T790M represents the only EGFR-resistance mutation, only one-third of crizotinib-resistant cases have a genetic alteration of ALK itself. The remaining cases of crizotinib-resistance are thought to arise through several different mechanisms.[6]

Tumorigenesis is not only dependent on the properties of cancer cells but also on the interactions with the immune system.[7,8] The interaction of programmed cell death–ligand 1 (PD-L1, also known as B7-H1 or CD274) expressed on antigen-presenting cells and parenchymal cells and its receptor programmed cell death–1 (PD-1, also known as CD279) on T cells is a physiologic mechanism that underlies escape from immune activity.[9] PD-L1 is also expressed in tumor cells, resulting in inhibition of the immune response to tumor cells and consequent facilitation of tumor progression. Approximately 24.8 to 69.2% of NSCLC were found to express PD-L1.[8-10] Thus, PD-L1 inhibition was introduced as a cancer treatment for

NSCLC and resulted in survival improvement in these patients.[11,12]

PD-L1 is more likely to be expressed in ALK-positive NSCLC than in EGFR/KRAS/ALK wild-type NSCLC (60% vs. 24%);[10] however, little is known about the role of the PD-1/PD-L1 pathway in ALK-positive NSCLC. Recently, Ota et al. reported that PD-L1 expression is induced by echinoderm microtubule-associated protein-like 4 (EML4)/ALK oncoprotein via downstream signaling pathways in NSCLC.[9] The influence of the PD-1/PD-L1 pathway on the resistance of ALK-positive NSCLC to ALK inhibitors, however, has yet to be defined. Here, we investigated alterations in PD-L1 expression after acquisition of resistance to ALK inhibitor in ALK-positive NSCLC.

MATERIALS AND METHODS

Patients and samples

We collected tumor tissues from 26 patients with metastatic NSCLC with ALK translocation from the Seoul National University Hospital from 2010 to 2014. Eleven specimens were biopsied before ALK inhibitor treatment, and 16 specimens were acquired after resistance developed to the ALK inhibitor crizotinib. Clinical and histological data were reviewed retrospectively. This study was approved by the Institutional Review Board at Seoul National University Hospital (H-1505-011-667).

Immunohistochemistry

Individual biopsy blocks were sectioned into 4-μm slices using a microtome and mounted on silanated slides. The sections were dewaxed in xylene and rehydrated using graded alcohol. Next, antigen retrieval was performed. Commercially available primary antibodies were used according to the manufacturer's instructions (anti-PD-L1 [E1L3N] XP, rabbit monoclonal, Cell Signaling Technology, Danvers, MA; anti-CD8, rabbit monoclonal, clone SP16, 1:100 dilution, Neomarkers, Fremont, CA; anti-FOXP3, mouse monoclonal, clone 236A/E7, 1:100 dilution, Abcam, Cambridge, UK; and anti-CD3, rabbit polyclonal, 1:100 dilution, DAKO, Glostrup, Denmark). Antibody binding was detected using

avidin-biotinperoxidase complex (Universal Elite ABC Kit; Vectastain; Vector Laboratories, Burlingame, CA) for 10 min, followed by development with diaminobenzidine tetrahydrochloride solution (Kit HK 153-5K; Biogenex, San Ramon, CA) for 5 min and counterstaining with hematoxylin.

The ALK inhibitor-naïve and -resistant tumor samples were stained for PD-L1, PD-1, CD3, CD4, CD8, CD68, and FOXP3. The biopsy slides were scanned using ScanScope XT (Aperio Technology, Vista, CA). The densities of the positively stained tumor-infiltrating lymphocytes (TILs) were evaluated in the intratumoral areas using the image analysis system (ScanScope XT; Aperio Technology). Then, the numbers of PD-1-, CD3-, CD4-, CD8-, CD68-, and FOXP3-positive TILs per unit area (mm^2) were calculated and subjected to statistical analyses.

For PD-L1 expression analysis, the intensity of staining was evaluated according to the following scale: 0, no staining; 1, weak staining; 2, moderate staining; and 3, strong staining. The proportion of membranous and/or cytoplasmic staining in tumor cells expressing PD-L1 was determined. Two kinds of PD-L1 scoring systems were applied. One scoring system was the H-score, which was defined and calculated as the product of the intensity score (0, 1, 2, and 3) and the proportion, resulting in a score of 0-300, as previously described.[13,14] The other scoring system was also based on the intensity and proportion of tumor cells as follows: 0, negative; 1, weak or moderate in <10% of tumor cells; 2, moderate in ≥10% of tumor cells; and 3, strong (more intense than alveolar macrophages) in ≥10% of tumor cells. Cases with scores of 2 or 3 were deemed positive for PD-L1

expression.[15] Bivariate analysis was performed using this result. The immunohistochemical stain results were analyzed by two pathologists who were blinded to the patients' identities and clinical data.

Cell lines and reagents

NCI-H3122 cells were provided by Pasi A. Jänne (Dana-Farber Cancer Institute, Boston, MA), and NCI-H2228 cells were purchased from the American Type Culture Collection (ATCC; Manassas, VA). H3122 and H2228 cells were maintained in RPMI 1640 medium with gentamicin (GIBCO, Grand Island, NY) and supplemented with 10% fetal bovine serum (GIBCO). The cell lines were incubated at 37°C in a humidified atmosphere of 5% carbon dioxide. Crizotinib and alectinib (CH-5424802) were purchased from Selleck Chemicals (Houston, TX) and dissolved in dimethyl sulfoxide (Sigma Aldrich, St. Louis, MO) for experiments. Ceritinib (LDK378) was obtained from Active Biochem (Maplewood, NJ). ALK inhibitor-resistant cell lines (CR1, LR1, and CH1) were established by exposing parental H3122 cells to crizotinib, ceritinib, and alectinib, respectively, at doses of 100 nM to 1 μM. Double-resistant cell lines (CR1LR1 and CR1CH1) were generated by exposing the crizotinib-resistant cell line CR1 to ceritinib and alectinib, respectively. The subclonal resistant cell lines exhibited ≥5-fold greater IC_{50} values for ALK inhibitors than parental cells, as determined using the cell viability assay, and this phenotype was stable for at least 6 months without ALK

inhibitor treatment. To investigate serial changes in PD-L1 expression after exposure to ALK inhibitors in ALK-positive lung cancer cell lines, we treated H3122 and H2228 cells with crizotinib, ceritinib, and alectinib for 70 d, and then we measured PD-L1 expression.

Cell viability assays

NSCLC cells were grown at a density of 5,000 cells/well in 96-well plates in the presence or absence of crizotinib, ceritinib, or alectinib for 72 h, and cell proliferation was analyzed using the CCK-8 colorimetric assay (Dojindo). The absorbance was measured at 450 nm in an Eon™ Microplate Spectrophotometer (BioTek, Winooski, VT) using at least triplicate samples.

Western blotting

The cell lines were harvested and lysed for western blot analysis. Primary antibodies PD-L1 and GAPDH (Cell Signaling Technology) were used for immunoblotting. The blots were washed, transferred to freshly prepared enhanced Lumi-Light Western Blotting Substrate (Roche, Indianapolis, IN), and subjected to imaging analysis using an LAS-3000 imaging system (Fuji Photo Film Co., Stamford, CT).

Flow cytometry

Cells (2×10^5) were separated into aliquots and placed into assay tubes. Then, 2 mL of fluorescence-activated cell sorting (FACS) buffer was added to each tube and rinsed by centrifugation twice. Cells were resuspended in 100 μl FACS buffer and then stained with mouse anti-human PD-L1 (MIH1, BD Pharmingen™) or a mouse IgG1 isotype control for 30 min on ice in staining buffer (2% BSA and 0.01% sodium azide). Analysis was conducted using a FACSCalibur instrument (BD Biosciences, San Jose, CA) with CELLQuest software (BD Biosciences) or Flow Jo software (Tree Star Inc., Ashland, OR).

Direct sequencing for mutations

Genomic DNA was extracted using the GenExTM Blood/Cell/Tissue kit (Geneall Biotechnology, Seoul, Korea) according to the manufacturer's protocol. Exons of ALK, EGFR, and KRAS were amplified from genomic DNA using the High Fidelity plus PCR system (Roche, Indianapolis, IN) and sequenced bi-directionally by Sanger dideoxynucleotide sequencing with primers as described previously.[16,17] Direct sequencing was performed with the ABI3730XL DNA analyzer (Applied Biosystems, Foster City, CA).

Quantitative PCR

Total RNA was collected from cultured cells using the Pure Link RNA mini kit

(Invitrogen). The cDNA was synthesized with SuperScript Ⅲ reverse transcriptase using random hexamer primers (Invitrogen). β-actin expression was used as an internal reference to normalize input cDNA. The ratios of the expression levels of each gene to that of the reference gene were calculated. The following primer sequences were used for quantitative PCR: PD-L1-F, 5'-TGG CAT TTG CTG AAC GCA TTT-3'; PD-L1-R, 5'-TGC AGC CAG GTC TAA TTG TTT T-3'; β-actin-F, 5'-CAA TGA GCT GCG TGT GGC T-3'; and β-actin-R, 5'-TAG CAC AGC CTG GAT AGC AA-3'. All experiments were repeated two times with similar results.

RNA sequencing

RNA sequencing was performed on NCI-H3122 and ALK inhibitor-derived cell lines using the Illumina TruSeq RNA sample prep kit v2 (Illumina, San Diego, CA). Quality and quantity of the library were measured using Bioanalyzer and Qubit. Sequencing of the transcriptome library was carried out using the paired-end mode of the TruSeq Rapid SBS kit (Illumina). Reads from FASTQ files were mapped against the hg19 human reference genome using TopHat2. Quantification of gene expression was performed, and differentially expressed genes were identified using the Tophat2–cufflink–cuffdiff axis.[18] Differentially expressed genes were selected and analyzed according to Gene Ontology (GO) classification, with GO searches using Gene Ontology Consortium (http://www.geneontology.org/) and ToppGene Suite

(http://toppgene.cchmc.org/).[19] We determined the representative pathways using Kyoto Encyclopedia of Genes and Genomes (KEGG) mapper[20]. In addition, fusion genes were detected by RNA sequencing and visualized in genomic regions using the Integrative Genomics Viewer tool.

Statistical analysis

The independent *t*-test was used to compare differences in densities of immune cell markers and PD-L1 H-score before and after acquisition of crizotinib resistance. The Mann-Whitney U-test was also used to compare PD-L1 H-score before and after acquisition of crizotinib resistance. The PD-L1 score (0, 1, 2, and 3) and positivity (negative and positive) before and after acquisition of crizotinib resistance were analyzed by Fisher's exact test and by linear-by-linear association. Two-sided *p*-values <0.05 were considered to indicate statistical significance. All statistical analyses were performed using SPSS statistics software, version 20 (IBM Corp., Armonk, NY).

RESULTS

Patients and tumor characteristics

The baseline characteristics of the patients are provided in Table 1. Twenty-six ALK-positive NSCLC patients (11 ALK inhibitor-naïve and 15 ALK inhibitor-resistant patients) were included in the present study. The median age at the time of biopsy was 53 years (range, 14 to 71), and most patients (92.3%) had pathologic diagnosis of adenocarcinoma. No significant differences in the baseline clinicopathologic characteristics between the two groups were noted. All ALK inhibitor-resistant patients underwent biopsy when the disease had progressed following crizotinib treatment. The median line of chemotherapy when ALK inhibitor was treated was second line (range, 1st–4th) for crizotinib. The overall response rate was 80.0%, and the median time-to-progression was 12.0 months (95% CI, 9.521–14.479).

Comparison of PD-L1 in pre-treatment and post-treatment tumor specimens

The expression of PD-L1 was compared between the tumor specimens before treatment and after treatment with ALK inhibitors using immunohistochemistry. Representative images for PD-L1 expression that were scored as 0, 1, 2, and 3 are shown in Figure 1. The mean PD-L1 H-score was 6.5 in pre-treatment samples and

35.0 in post-treatment samples, and the fold difference between these two measurements was 5.42 (p=0.163, Figure 2A). The results of analysis with another PD-L1 score (0-3) and PD-L1 positivity are shown in Figure 2B and 2C. Despite the lack of statistical significance, more samples from post-treatment patients were positive for PD-L1 than samples from pre-treatment patients (3 [20.0%] vs. 0 [0.0%] patients, p=0.175).

Table 1. Baseline characteristics of patients and patient outcomes after crizotinib treatment

	Total	Time of biopsy		*p*-value
		Pre-treatment	Post-treatment	
Total (n)	26	11	15	
Age (y)				0.178
<60	19 (73.1%)	10 (90.9%)	9 (60.0%)	
≥60	7 (26.9%)	1 (9.1%)	6 (40.0%)	
Sex				0.178
M	7 (26.9%)	1 (9.1%)	6 (40.0%)	
F	19 (73.1%)	10 (90.9%)	9 (60.0%)	
Smoking history				0.356
Never-smoker	21 (80.8%)	10 (90.9%)	11 (73.3%)	
Smoker	5 (19.2%)	1 (9.1%)	4 (26.7%)	
Histology				1.000
Adenocarcinoma	24 (92.3%)	10 (90.9%)	14 (93.3%)	
Non-small cell carcinoma, NOS	2 (7.7%)	1 (9.1%)	1 (6.7%)	
Outcome following crizotinib treatment[*]				
Best response[†]	Partial response		10 (66.7%)	
	Stable disease		2 (13.3%)	
	Progressive disease		0 (0.0%)	
	Unknown[‡]		3 (20.0%)	
Time-to-progression (months)			12.0 (95% CI, 9.521–14.479)	

NOS, not otherwise specified; CI, confidence interval
[*]Among post-treatment samples
[†]Determined by the Response Evaluation Criteria in Solid Tumors
[‡]Patients treated with crizotinib in other hospitals and did not have available information about the response to crizotinib

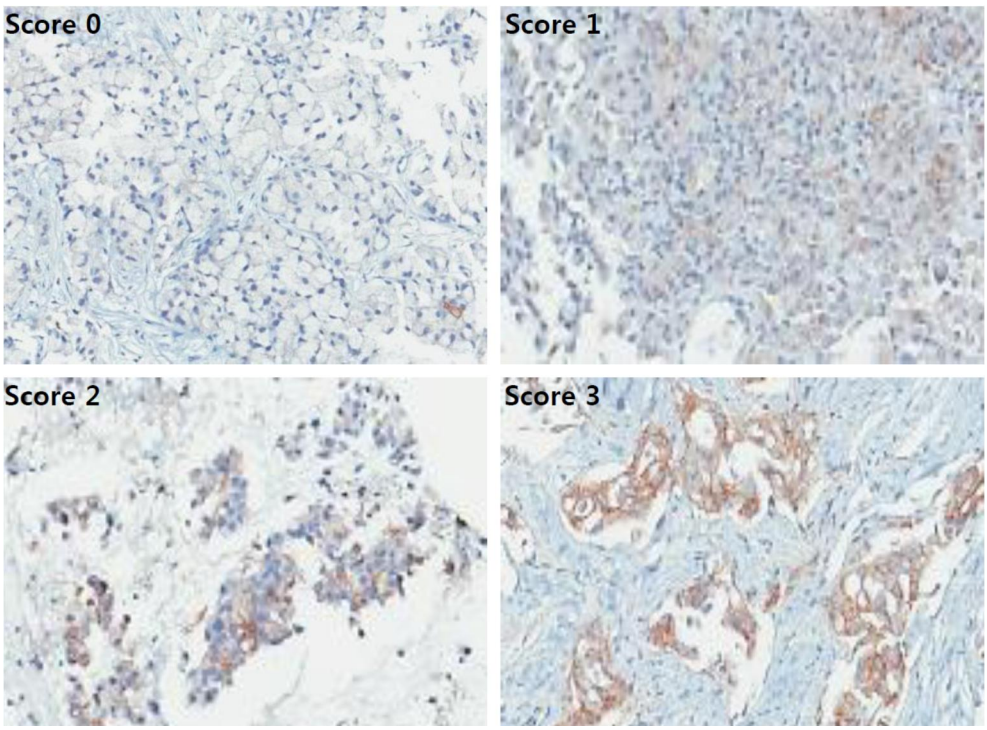

Figure 1. Representative images of PD-L1 immunohistochemistry in NSCLC patients (original magnification ×400). PD-L1 score was graded as absent (score 0), weak (score 1), moderate (score 2), or strong (score 3). A score of 2 or 3 was deemed positive for PD-L1 expression.

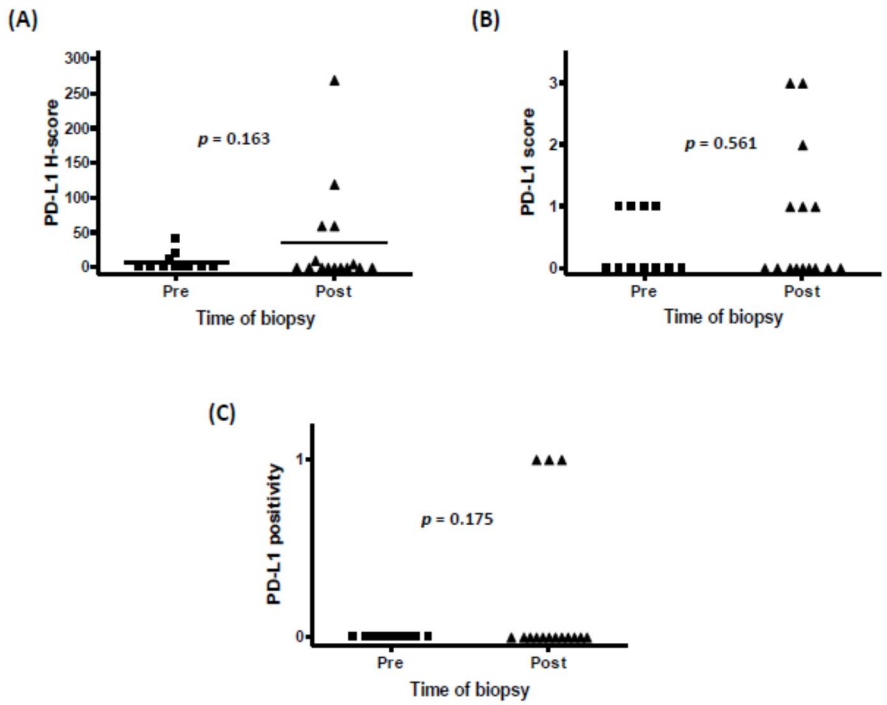

Figure 2. Changes in PD-L1 before and after crizotinib treatment in ALK-positive NSCLC tumor tissues based on (A) H-score, (B) PD-L1 score (0, 1, 2, 3), and (C) positivity.

Comparison of expression of lymphocyte markers in TILs between pre- and post-treatment NSCLC tumor specimens

The expression of immune markers CD3, CD4, CD8, FOXP3, CD68, and PD-1 in TILs is described in Table 2. No significant differences in the expression of immune markers between pre- and post-treatment tumor tissues were detected, except for CD68. The mean numbers of CD68/mm^2 were 181.6±115.4 in pre-treatment tumor samples and 90.8±48.9 in post-treatment tumor samples (p=0.030). In addition, expression of CD3, CD8, and PD-1 tended to be lower in the post-treatment group compared to the pre-treatment group samples; however, this difference was not significant.

Table 2. The numbers of immune marker-positive TILs/mm^2 in the pre- and post-treatment tumor specimens.

	Pre-treatment (n=11)	Post-treatment (n=15)	*p*-value
CD3, mean±SD	500.7±244.5	366.0±149.3	0.128
CD4, mean±SD	247.6±151.5	257.5±167.6	0.878
CD8, mean±SD	263.6±126.4	186.7±121.2	0.129
FOXP3, mean±SD	58.0±42.1	46.1±52.7	0.541
CD68, mean±SD	181.6±115.4	90.8±48.9	0.030
PD-1, mean±SD	6.1±8.8	3.6±4.9	0.363

SD, standard deviation

Changes in PD-L1 protein levels before and after acquisition of ALK inhibitor resistance in ALK-positive lung cancer cell lines

Growth inhibition rates were used to calculate the IC_{50} for each cell line (Table 3 and Figure 3). We investigated the resistance mechanisms, including secondary mutations in ALK, EGFR, and KRAS, and found no mutations in these cell lines. *In vitro* clones with resistance to ALK inhibitors were selected by growing H3122 cells in increasing concentrations of ALK inhibitors to a final concentration of 1 μM, and cells were maintained under these conditions for ≥6 months. PD-L1 expression in H3122 and sublines was analyzed by immunoblotting. Markedly increased PD-L1 expression was observed in the cell lines as resistance to ALK inibitors was acquired (Figure 4). Furthermore PD-L1 expression in the double-resistant cell lines was much higher than that in the single-resistant cell lines.

Table 3. ALK inhibitor-resistant cell lines and resistance mutation status.

Cell Line[1]	IC_{50} (μM)			Resistance mutation		
	Crizotinib	Ceritinib	Alectinib	ALK mutation	EGFR mutation	KRAS mutation
H3122	0.15	0.05	0.02	WT	WT	WT
H3122CR1	0.95	0.35	>5	WT	WT	WT
H3122LR1	5.49	1.21	6.71	WT	WT	WT
H3122CH1	1.39	0.80	>5	WT	WT	WT
H3122CR1CH1	4.51	1.01	9.32	WT	WT	WT
H3122CR1LR1	4.45	1.16	>5	WT	WT	WT

WT, wild type

All cell lines have ALK translocation

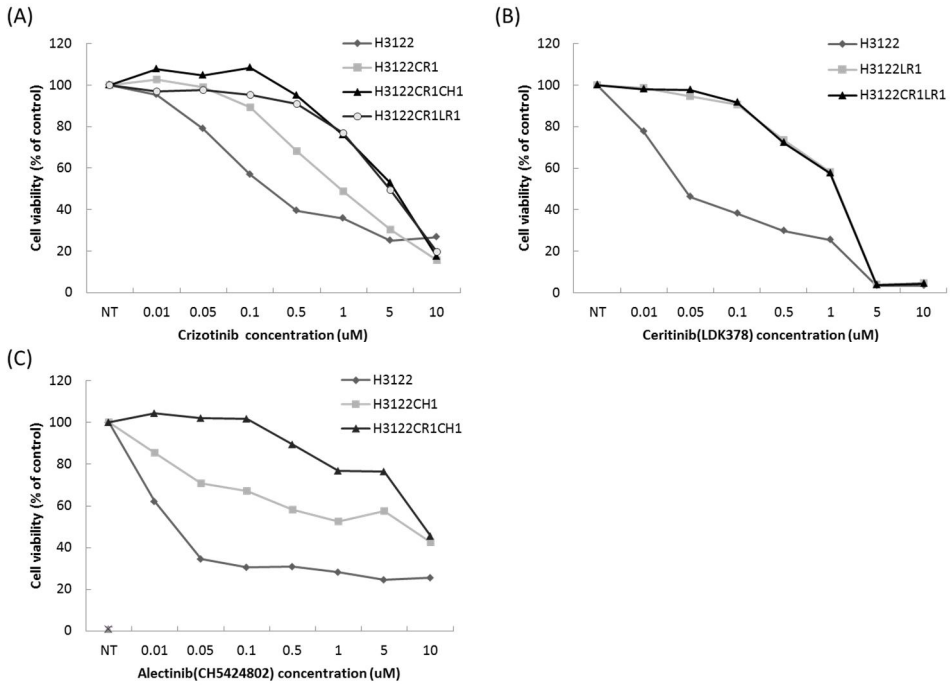

Figure 3. Cell viability assays with H3122 and subclonal resistant cell lines.

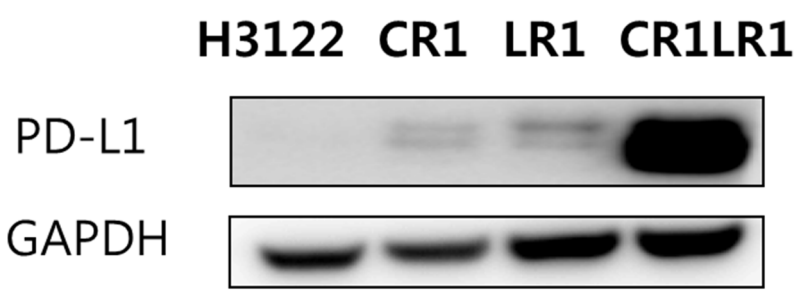

Figure 4. PD-L1 protein levels in the parental H3122 and its subclonal cell lines with single- and double-resistant cell lines.

Changes in PD-L1 surface protein levels before and after acquisition of ALK inhibitor resistance in ALK-positive lung cancer cell lines

The panel of lung cancer cell lines harboring the ALK translocation was examined for cell surface PD-L1 expression by flow cytometry before and after the establishment of ALK inhibitor resistance (Figure 5). The expression of surface PD-L1 as assessed by the median fluorescence intensity was increased 1.3- to 2.5-fold in CR1, LR1, and CH1 cell lines compared with levels in the parental cell line. Following the establishment of the double resistance to ALK inhibitors, the CR1LR1 and CR1CH1 cell lines expressed markedly higher levels (3.9- to 5.2-fold increase) of PD-L1 than their parental line counterparts.

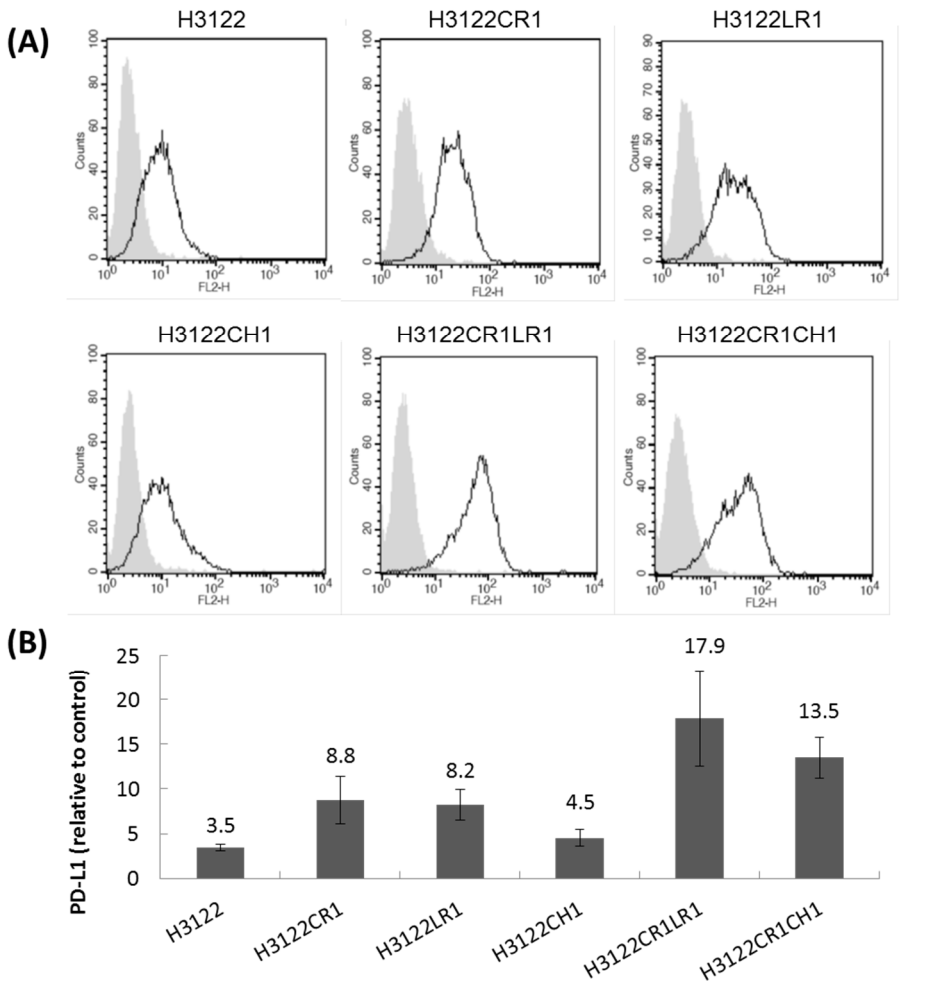

Figure 5. PD-L1 surface protein levels in cell lines after acquiring single and double resistance to ALK inhibitors by FACS analysis. (A) Histograms depict PD-L1 expression. (B) Mean fluorescence intensity (MFI) was determined by gating on live cells. The error bars indicate the standard deviation.

Changes in PD-L1 mRNA levels before and after acquisition of ALK inhibitor resistance in ALK-positive lung cancer cell lines

The changes in PD-L1 mRNA levels after acquisition of resistance to ALK inhibitors were assessed by quantitative PCR. In CR1, LR1, and CH1 cell lines, the levels of PD-L1 mRNA were increased by 2.5-, 2.4-, and 4.9-fold, respectively. Following acquisition of double resistance to ALK inhibitors, lung cancer lines expressed 7.4- to 9.8-fold higher levels of PD-L1 than their parental line counterparts (Figure 6).

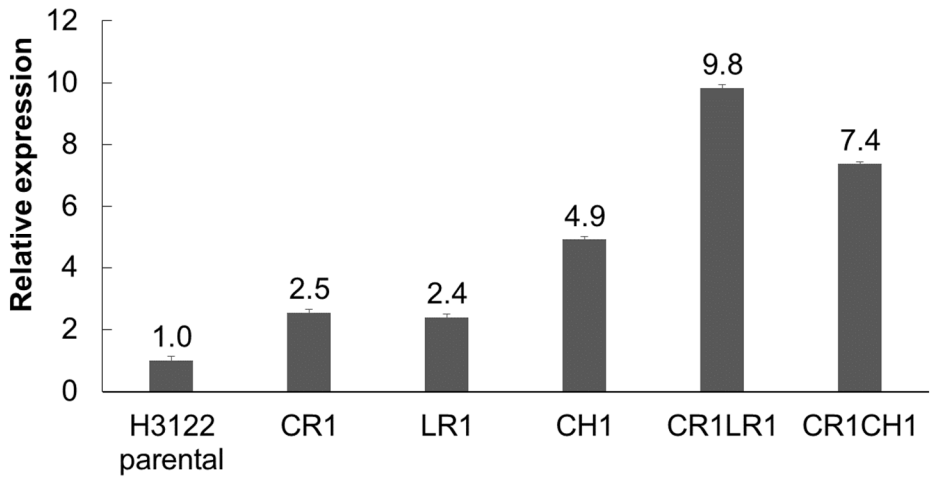

Figure 6. PD-L1 mRNA levels in parental H3122 cells and subclonal cell lines after acquisition of single and double resistance to ALK inhibitors. The error bars indicate the standard deviation.

Sequential changes in cell surface PD-L1 after ALK inhibitor treatment in ALK-positive cell lines

As PD-L1 expression is downregulated by ALK inhibition, we tested whether PD-L1 expression initially decreases after ALK inhibitor treatment and thereafter increases after establishment of resistance. We investigated PD-L1 changes over time as ALK-positive lung cancer cell lines H3122 and H2228 developed resistance to ALK inhibitors. Figure 7 shows serial changes of PD-L1 expression by flow cytometry following treatment with the ALK inhibitors crizotinib, ceritinib, or alectinib. Although the initial reduction in PD-L1 expression was not prominent, PD-L1 expression increased after 50 d of exposure of the cell lines to the ALK inhibitors.

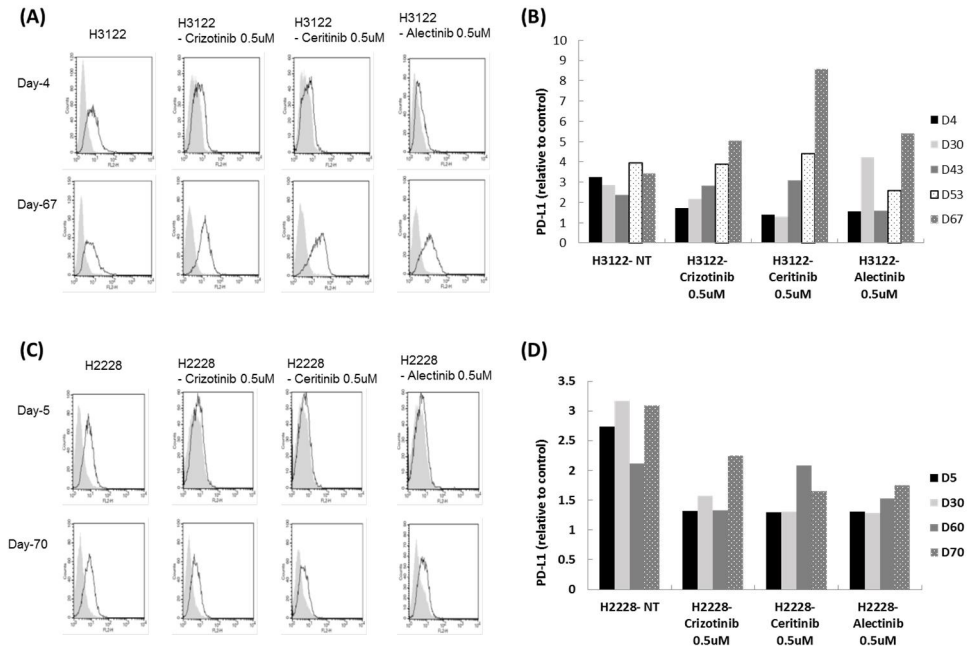

Figure 7. Sequential changes of PD-L1 by flow cytometry following treatment with ALK inhibitors crizotinib, ceritinib, or alectinib in (A and B) H3122, and (C and D) H2228. B and D show MFI for each cell line. NT, not treated.

Transcriptome profile

RNA sequencing was performed on the following six cell lines: H3122 parental, CR1, LR1, CH1, CR1LR1, and CR1CH1. The mean read count was 6.7×10^7 (standard deviation, $\pm 7.0 \times 10^6$). The gene expression levels were estimated as fragments per kilobase of transcript per million fragments mapped (FPKM) values. We excluded genes that were not matched to reference genes or nameless, and at least one of the FPKM values for each cell line was 0, to avoid erroneous detection. In total, 16,984 genes were analyzed. Figure 8 shows the heatmap of differential expression of these 16,984 genes in H3122 and sublines. CR1 and CH1 shared similar features of gene expression, and the double-resistant CR1LR1 and CR1CH1 cells also shared common features of gene expression.

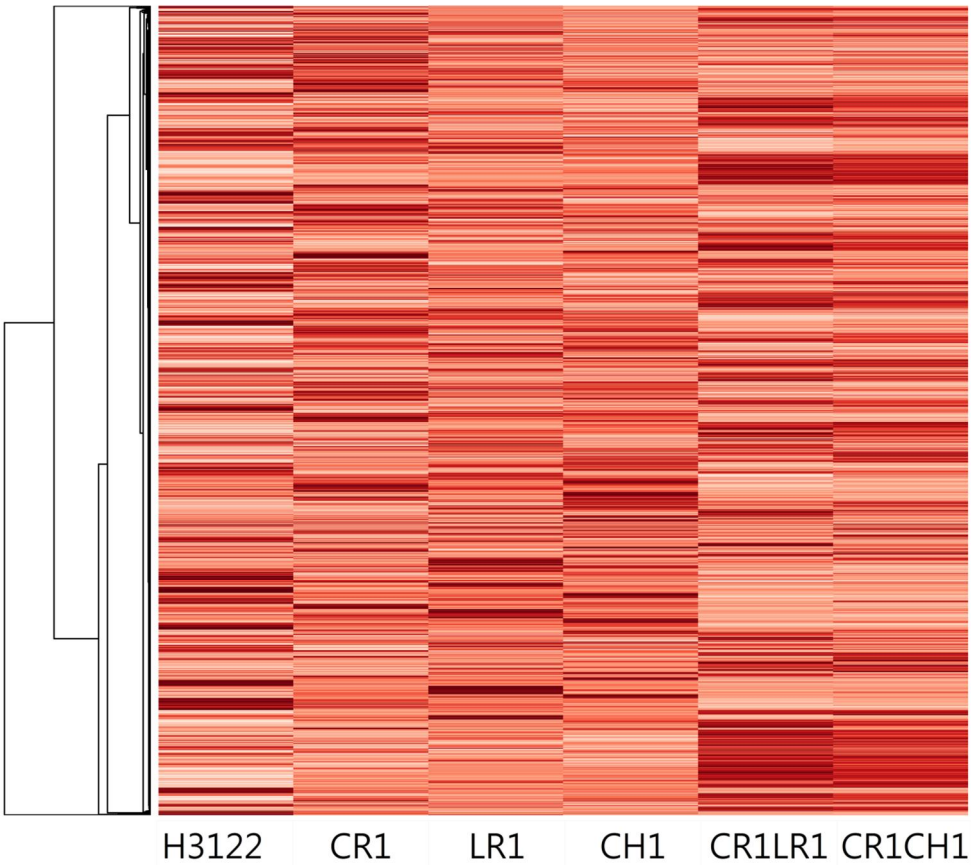

Figure 8. The heatmap of gene expressions of whole transcriptome analysis for H3122 and ALK inhibitor-resistant sublines. Rows of each heat map correspond to genes sorted according to clustering (16,984 genes).

To evaluate differently expressed genes in the resistant lines compared to the H3122 parental line, we divided the cell lines into the following three groups according to the degree of resistance: H3122 parental, R1 (CR1, LR1, and CH1), and R2 (CR1LR1, and CR1CH1) groups. We estimated the mean FPKM values for each group. Then, we selected 739 genes that were expressed differently with an absolute $\log_2$ fold change in FPKM values >2 between H3122 parental and either R1 or R2. Log_2 fold changes of the differentially expressed genes are illustrated with a heatmap (Figure 9).

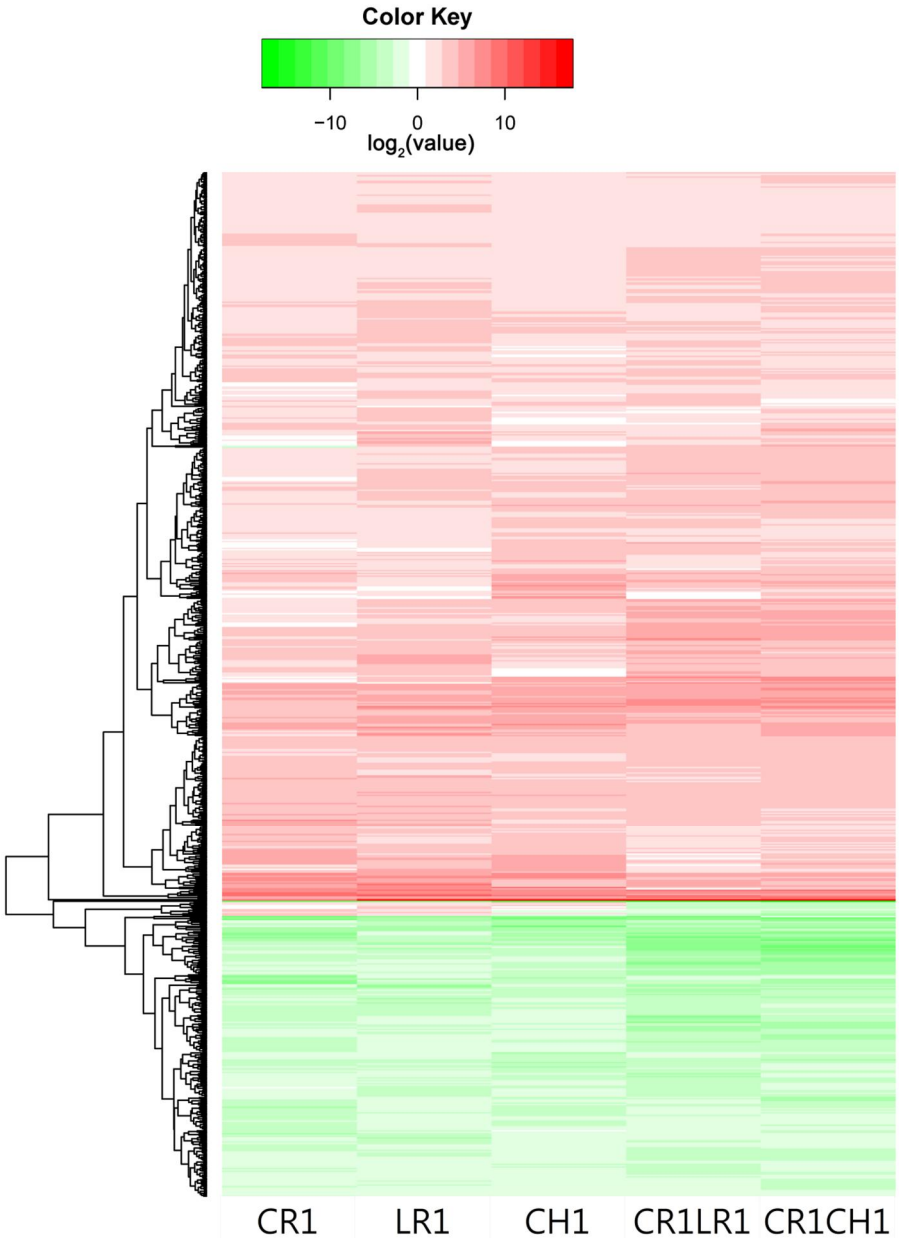

Figure 9. The heatmap illustrates expression of genes with an absolute $\log_2$ fold change in FPKM >2 in R1 (CR1, LR1, and CH1) and R2 (CR1LR1, and CR1CH1) groups compared to H3122 cell lines. Rows of each heat map correspond to genes sorted according to clustering (739 genes).

We then selected the top 20 ranked genes in each comparison (parental vs. R1 and parental vs. R2). Log_2 fold changes of mean FPKM values in each group compared to the parental H3122 cell line are shown in Figure 10 and Table 4. Eight genes were among the top 20 absolute log_2 fold changes in both the R1 and R2 groups, indicating the validity of these results and highlighting the importance of these genes.

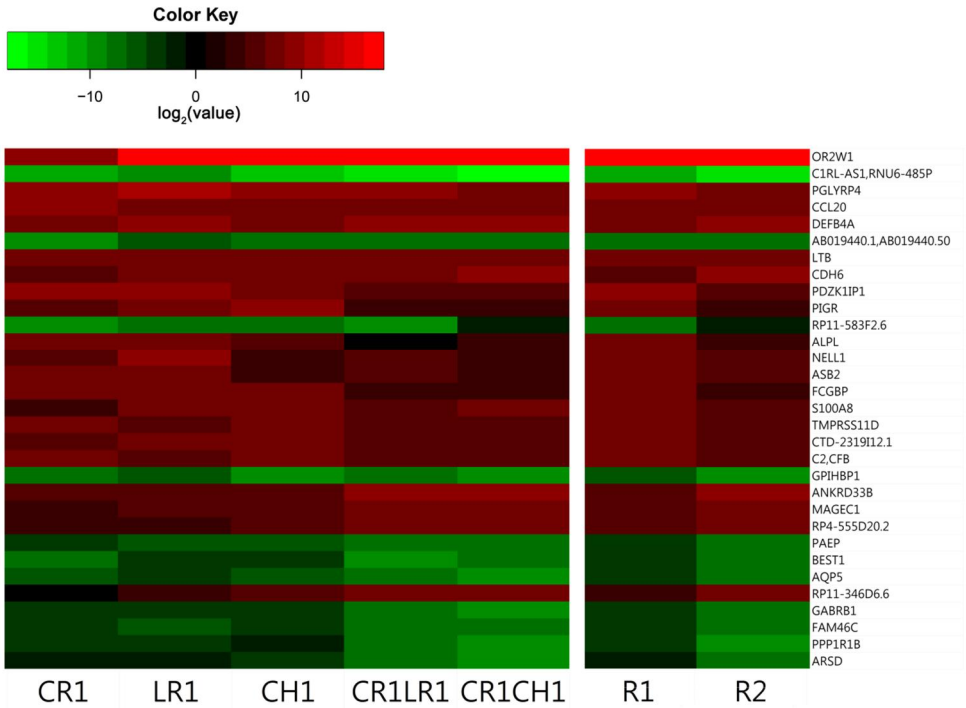

Figure 10. The heatmap of $\log_2$ fold changes of gene expression in ALK inhibitor-resistant cell lines compared to parental H3122 cell lines. The image represents the top 20 absolute $\log_2$ fold changes in each comparison (H3122 vs. R1 and H3122 vs. R2; total: 32 genes)

Table 4. Thirty-two genes that were differently expressed in the R1 (CR1, LR1, and CH1) or R2 (CR1LR1, and CR1CH1) groups compared to the parental H3122 cell line are described with the top 20 ranking genes with an absolute $\log_2$ fold change.

Symbol	Full name	Function	Group with top 20 $\pm\log_2$ FC	Log_2 FC	
				R1	R2
OR2W1	Olfactory Receptor Family 2 Subfamily W Member 1	G-protein-coupled receptor activity, olfactory receptor activity	Both	16.66	17.33
C1RL-AS1, RNU6-485P	C1RL Antisense RNA 1, RNA, U6 Small Nuclear 485, Pseudogene	Unknown	Both	-10.95	-15.42
PGLYRP4	Peptidoglycan Recognition Protein 4	Peptidoglycan binding, defense response to Gram-positive bacteria, innate immune response	Both	9.77	8.04
CCL20	C-C Motif Chemokine Ligand 20	Extracellular region, T cell migration, cell chemotaxis, immune response	Both	7.98	7.12
DEFB4A	Defensin Beta 4A	Chemotaxis, immune response	Both	7.8	8.62
AB019440.1, AB019440.50	ENSG00000211945(Immunoglobulin Heavy Variable 1-18 (IGHV1-18), ENSG00000271201	Unknown	Both	-7.09	-8.03
LTB	Lymphotoxin Beta	Plasma membrane, immune response	Both	6.91	8.05
CDH6	Cadherin 6	Plasma membrane, adherens junction organization	Both	6.52	8.69
PDZK1IP1	PDZK1 Interacting Protein 1	Extracellular exosome, integral component of membrane	R1	8.54	5.98
CD177	CD177 Molecule	Plasma membrane, protein binding, leukocyte migration	R1	7.87	3.43
PIGR	Polymeric Immunoglobulin Receptor	Extracellular exosome, epidermal growth factor receptor signaling pathway, immunoglobulin transcytosis in epithelial cells mediated by polymeric immunoglobulin receptor	R1	7.85	3.04
RP11-583F2.6	Uncharacterized LOC105371863	Unknown	R1	-7.82	-2.17
ALPL	Alkaline Phosphatase, Liver/Bone/Kidney	Extracellular exosome, alkaline phosphatase activity	R1	7.56	3
NELL1	Neural EGFL Like 1	Cell differentiation, extracellular region, negative regulation of osteoblast proliferation	R1	7.43	4.91

Table 4. (continued)

Symbol	Full name	Function	Group with top 20 $\pm \log_2$FC	Log_2 FC	
				R1	R2
ASB2	Ankyrin Repeat and SOCS Box Containing 2	Intracellular signal transduction, protein polyubiquitination, myoblast differentiation	R1	6.98	5.18
FCGBP	Fc Fragment Of IgG Binding Protein	Extracellular exosome, protein binding	R1	6.95	3.95
S100A8	S100 Calcium Binding Protein A8	Extracellular exosome, protein binding, inflammatory response, chemokine production, cytoskeleton, innate immune response, leukocyte migration involved in inflammatory response	R1	6.9	6.31
TMPRSS11D	Transmembrane Protease, Serine 11D	Extracellular exosome, proteolysis, respiratory gaseous exchange	R1	6.86	5.64
CTD-2319I12.1	WAP Four-Disulfide Core Domain 21, Pseudogene (WFDC21P)	Unknown	R1	6.75	5.92
C2, CFB	Complement Component 2, Complement Factor B	Protein binding, extracellular exosome, complement activation, phosphatidylinositol 3-kinase complex, plasma membrane	R1	6.6	5.94
GPIHBP1	Glycosylphosphatidylinositol Anchored High Density Lipoprotein Binding Protein 1	Anchored component of external side of plasma membrane, cholesterol homeostasis	R2	-6.34	-8.56
ANKRD33B	Ankyrin Repeat Domain 33B	Unknown in *Homo sapiens*	R2	6.28	9.44
MAGEC1	MAGE Family Member C1	Protein binding	R2	5.19	7.68
RP4-555D20.2	ENSG00000261786	Unknown	R2	4.77	7.18
PAEP	Progestagen-Associated Endometrial Protein	Apoptotic process, positive regulation of granulocyte macrophage colony-stimulating factor production, positive regulation of interleukin-13 secretion, positive regulation of interleukin-6 secretion	R2	-4.54	-7.2
BEST1	Bestrophin 1	Plasma membrane, ion transmembrane transport	R2	-4.37	-8.29
AQP5	Aquaporin 5	Water channel activity, plasma membrane, cellular water homeostasis	R2	-4.24	-8.02

Table 4. (continued)

Symbol	Full name	Function	Group with top 20 $\pm \log_2$FC	Log_2 FC	
				R1	R2
RP11-346D6.6	Long Intergenic Non-Protein Coding RNA 1468 (LINC01468)	Unknown	R2	4.18	7.12
GABRB1	Gamma-Aminobutyric Acid Type A Receptor Beta1 Subunit	GABA-A receptor complex, cell junction, ion transmembrane transport	R2	-3.85	-7.56
FAM46C	Family With Sequence Similarity 46 Member C	Unknown in *Homo sapiens*	R2	-3.77	-7.5
PPP1R1B	Protein Phosphatase 1 Regulatory Inhibitor Subunit 1B	Cytosol, D1-5 dopamine receptor binding, intracellular signal transduction, protein kinase inhibitor activity	R2	-3.04	-8.74
ARSD	Arylsulfatase D	Arylsulfatase activity, extracellular exosome, post-translational protein modification	R2	-2.43	-8.06

FC, Fold change

Gene expression of representative immune checkpoint genes and common oncogenic pathways, including ALK and lung adenocarcinoma-related genes reported by The Cancer Genome Atlas, were identified and described in Tables 5 and 6.

Table 5. FPKM values of immune checkpoint genes in H3122 and ALK inhibitor-resistant cell lines.

Symbol	Cell lines					
	H3122	CR1	LR1	CH1	CR1LR1	CR1CH1
CD274 (PDL1)	1.26	4.82	2.20	4.76	13.72	12.38
PDCD1 (PD1)	0.08	0.01	0.00	0.00	0.00	0.00
PDCD1LG2 (PDL2)	0.00	0.07	0.03	0.00	0.10	0.19
PDCD2 (PD2)	71.13	57.20	42.92	57.10	76.55	64.55
LAG3	0.10	0.35	1.04	0.40	0.08	0.07
TIM3 (HAVCR2)	4.84	5.98	7.99	9.17	4.53	5.16
CTLA4	0.00	0.00	0.02	0.00	0.00	0.00

Genes with FPKM values of 0 were included for reference.

Table 6. FPKM values of ALK, other common oncogenic pathways, and lung adenocarcinoma-related genes according to The Cancer Genome Atlas.

Symbol	Cell lines					
	H3122	CR1	LR1	CH1	CR1LR1	CR1CH1
ALK	12.17	16.04	8.93	20.18	6.55	5.97
EGFR	17.04	22.89	9.58	10.79	15.14	17.95
KRAS	11.38	16.56	12.21	15.73	21.23	15.65
BRAF	4.95	6.08	4.11	3.13	4.00	2.80
ERBB2	17.70	31.18	28.54	20.54	22.99	15.48
KIT	0.23	0.37	0.92	0.75	0.75	0.63
MET	41.23	46.66	19.65	29.18	43.77	43.15
MAP2K1	14.63	22.11	16.96	31.92	34.09	35.34
PIK3CA	3.11	3.58	3.04	4.87	8.33	6.60
TP53	54.02	45.18	45.29	38.04	40.68	41.01
STK11	42.77	50.77	41.65	47.45	37.58	45.95
KEAP1	25.47	23.20	25.94	21.99	42.22	37.29
NF1	6.62	6.68	5.64	7.01	10.32	7.48
SMARCA4	79.57	87.30	79.25	60.40	79.75	60.12
RBM10	19.08	17.44	16.99	16.46	18.23	18.88
RB1	14.75	9.85	8.89	11.15	15.18	18.06
U2AF1	225.89	164.33	167.45	130.37	229.07	233.62
RIT1	9.07	24.83	15.54	19.71	14.78	16.55
CDKN2A	0.06	0.39	0.00	0.07	0.67	0.12
SETD2	13.27	12.48	13.51	11.21	12.92	10.42
ARID1A	29.64	21.44	33.14	19.18	42.77	33.71
MGA	4.19	3.83	3.69	3.96	5.01	4.17

Genes with FPKM values of 0 were included for reference.

GO enrichment analysis was performed using the ToppGene database. The analysis was performed with genes that were differentially expressed by >4 or <-4 $\log_2$ fold changes to explore the relationship between the resistance and the biological processes and pathways for stricter analysis. Table 7 shows the specific biological processes ordered according to statistical significance. Table 8 shows the pathways enriched in the differentially expressed gene sets.

Table 7. Top ten GO terms of differentially expressed genes with absolute $\log_2$ fold change of FPKM >4 ordered by statistical significance.

ID	GO terms	*Q*-value	Count	Genes
GO:0001816	Cytokine production	5.93E-03	31	CD83,UBASH3A,S100A8,S100A12,HEG1,SCGB1A1,CCL20,HSPA1A,HTR2B,BIRC3,IFI16,IL23A,CSF2,PRG2,IL1A,CYBA,SERPINB7,IL15,TNFRSF9,IL18,IL17C,PTAFR,BST2,PGLYRP4,CAMK4,NFAM1,PAEP,IRAK3,RORC,LTB,TNFAIP3
GO:0006955	Immune response	5.93E-03	52	IL32,TNIP3,RFTN2,CD83,UBASH3A,S100A8,S100A12,CCL28,PIGR,CCL20,MMP7,HSPA1A,BIRC3,IFI16,IFI27,IL23A,CSF2,PRG2,IL1A,STX11,IFI6,MX1,IL7R,CYBA,IL15,TNFRSF9,IL18,TNFSF10,PSMB9,PTAFR,CCL27,CFB,PTK6,DEFB4A,BST2,PLCL2,C2,IFI44L,DOCK2,PGLYRP4,CAMK4,TRIM31,GPR183,CAV1,LCN2,NFAM1,CXCL3,IRAK3,RORC,LTB,TNFAIP3,TNFRSF1B
GO:0051707	Response to other organism	5.93E-03	38	TNIP3,S100A8,S100A12,SCGB1A1,CCL20,MMP7,ALPL,IFI44,BIRC3,IFI16,IL23A,BPIFA2,CSF2,PRG2,ASB2,MX1,CYBA,CYP1A2,IL15,TNFRSF9,IL18,PSMB9,PTAFR,DEFB4A,BST2,IFI44L,FGFBP1,DOCK2,PGLYRP4,MUC5B,CAV1,LCN2,CXCL3,THBD,IRAK3,TNFAIP3,TNFRSF1B,CDK6
GO:0043207	Response to external biotic stimulus	5.93E-03	38	TNIP3,S100A8,S100A12,SCGB1A1,CCL20,MMP7,ALPL,IFI44,BIRC3,IFI16,IL23A,BPIFA2,CSF2,PRG2,ASB2,MX1,CYBA,CYP1A2,IL15,TNFRSF9,IL18,PSMB9,PTAFR,DEFB4A,BST2,IFI44L,FGFBP1,DOCK2,PGLYRP4,MUC5B,CAV1,LCN2,CXCL3,THBD,IRAK3,TNFAIP3,TNFRSF1B,CDK6
GO:0009607	Response to biotic stimulus	5.93E-03	39	TNIP3,S100A8,S100A12,SCGB1A1,CCL20,MMP7,ALPL,IFI44,BIRC3,IFI16,IL23A,BPIFA2,CSF2,PRG2,SMO,ASB2,MX1,CYBA,CYP1A2,IL15,TNFRSF9,IL18,PSMB9,PTAFR,DEFB4A,BST2,IFI44L,FGFBP1,DOCK2,PGLYRP4,MUC5B,CAV1,LCN2,CXCL3,THBD,IRAK3,TNFAIP3,TNFRSF1B,CDK6
GO:0001817	Regulation of cytokine production	3.46E-02	27	CD83,UBASH3A,HEG1,SCGB1A1,CCL20,HSPA1A,HTR2B,BIRC3,IFI16,IL23A,CSF2,PRG2,IL1A,CYBA,SERPINB7,IL15,TNFRSF9,IL18,IL17C,PTAFR,BST2,PGLYRP4,NFAM1,PAEP,IRAK3,LTB,TNFAIP3
GO:0007267	Cell-cell signaling	5.69E-02	41	LRRK2,FOXA2,CHRM3,CHRNB2,RYR2,SCN4B,SCN5A,CCL20,VIPR2,GDF15,BCAN,SNCAIP,WNT10A,SMO,RIMS1,SNCG,STX11,UNC13A,GABRB2,IL15,IL18,SNPH,TNFSF10,IL17C,MYT1,CEACAM6,CCL27,C2CD4C,GFAP,SV2B,BST2,PLCL2,SYP,SYT1,FGFBP1,CAMK4,PCDHB11,EDN2,LHX1,GPR68,LTB

Table 7. (continued)

ID	GO terms	*Q*-value	Count	Genes
GO:0009617	Response to bacterium	6.39E-02	25	TNIP3,S100A8,S100A12,SCGB1A1,CCL20,MMP7,ALPL,IL23A,BPIFA2,CSF2,PRG2,CYBA,CYP1A2,TNFRSF9,IL18,PTAFR,DEFB4A,PGLYRP4,MUC5B,CAV1,CXCL3,THBD,IRAK3,TNFAIP3,TNFRSF1B
GO:0001819	Positive regulation of cytokine production	8.03E-02	20	CD83,HEG1,CCL20,HSPA1A,HTR2B,BIRC3,IFI16,IL23A,CSF2,PRG2,IL1A,CYBA,SERPINB7,IL15,IL18,IL17C,PTAFR,NFAM1,PAEP,LTB
GO:0006952	Defense response	9.40E-02	49	SERPINA3,IL32,TNIP3,CD83,S100A8,S100A12,SCGB1A1,CCL20,MMP7,HSPA1A,BIRC3,IFI16,IFI27,IL23A,BPIFA2,PRG2,ASB2,IL1A,STX11,IFI6,MX1,CYBA,IL15,TNFRSF9,IL18,IL17C,PSMB9,PTAFR,CFB,PTK6,DEFB4A,BST2,C2,IFI44L,FGFBP1,DOCK2,PGLYRP4,CAMK4,TRIM31,MUC5B,CAV1,LCN2,NFAM1,CXCL3,GPR68,APOL3,IRAK3,TNFAIP3,TNFRSF1B

GO, gene ontology
Q values were estimated by Benjamini and Hochberg procedure to control the false discovery rate.

Table 8. Enriched pathways in the differentially expressed genes of absolute log2 fold change of FPKM >4 ordered by statistical significance

ID	Name	*Q* -value	Count	Genes
M5889	Ensemble of genes encoding extracellular matrix and extracellular matrix-associated proteins	2.27E-11	54	SERPINA3,ANXA8L1,S100A8,S100A12,PI3,SERPINA4,CCL28,LOXL4,MMP1,CCL20,MMP7,MMP10,COL4A1,COL4A2,COL5A1,SFTPB,GDF15,BCAN,MUC13,IL23A,CSF2,IGFBP3,IGFBP5,PRG2,SCUBE3,WNT10A,IL1A,FAM20A,CTSE,MEGF11,SERPINB7,PRSS1,IL15,IL18,TNFSF10,SPOCK1,IL17C,COL25A1,CCL27,NELL1,FREM2,CRISPLD1,FGF19,FGFBP1,INHBE,MUC5B,EDIL3,CXCL3,LGALS7,FSTL1,VWA5A,LOX,LTB,SERPINA5
M5885	Ensemble of genes encoding ECM-associated proteins including ECM-affiliated proteins, ECM regulators, and secreted factors	1.10E-08	41	SERPINA3,ANXA8L1,S100A8,S100A12,PI3,SERPINA4,CCL28,LOXL4,MMP1,CCL20,MMP7,MMP10,SFTPB,GDF15,MUC13,IL23A,CSF2,SCUBE3,WNT10A,IL1A,FAM20A,CTSE,MEGF11,SERPINB7,PRSS1,IL15,IL18,TNFSF10,IL17C,CCL27,FREM2,FGF19,FGFBP1,INHBE,MUC5B,CXCL3,LGALS7,FSTL1,LOX,LTB,SERPINA5
M5883	Genes encoding secreted soluble factors	3.60E-05	22	S100A8,S100A12,CCL28,CCL20,GDF15,IL23A,CSF2,SCUBE3,WNT10A,IL1A,MEGF11,IL15,IL18,TNFSF10,IL17C,CCL27,FGF19,FGFBP1,INHBE,CXCL3,FSTL1,LTB
200309	Rheumatoid arthritis	8.07E-03	9	ATP6V1C2,MMP1,CCL20,IL23A,CSF2,IL1A,IL15,IL18,LTB
83051	Cytokine-cytokine receptor interaction	1.10E-02	15	CCL28,CCL20,IL23A,CSF2,IL1A,IL7R,IL15,TNFRSF9,IL18,TNFSF10,CCL27,INHBE,CXCL3,LTB,TNFRSF1B
M3468	Genes encoding enzymes and their regulators involved in the remodeling of the extracellular matrix	4.17E-02	13	SERPINA3,PI3,SERPINA4,LOXL4,MMP1,MMP7,MMP10,FAM20A,CTSE,SERPINB7,PRSS1,LOX,SERPINA5
730306	Assembly of collagen fibrils and other multimeric structures	4.80E-02	6	LOXL4,MMP7,COL4A1,COL4A2,COL5A1,LOX

Q values were estimated by Benjamini and Hochberg procedure to control the false discovery rate.

The differentially expressed genes with a >2 or <-2 $\log_2$ fold change were assessed using the KEGG mapper tool. Representative pathways related to the differentially expressed genes include cancer, cytokine-cytokine receptor interactions, and extracellular matrix-receptor interactions. These pathways are illustrated in Figures 11, 12, and 13.

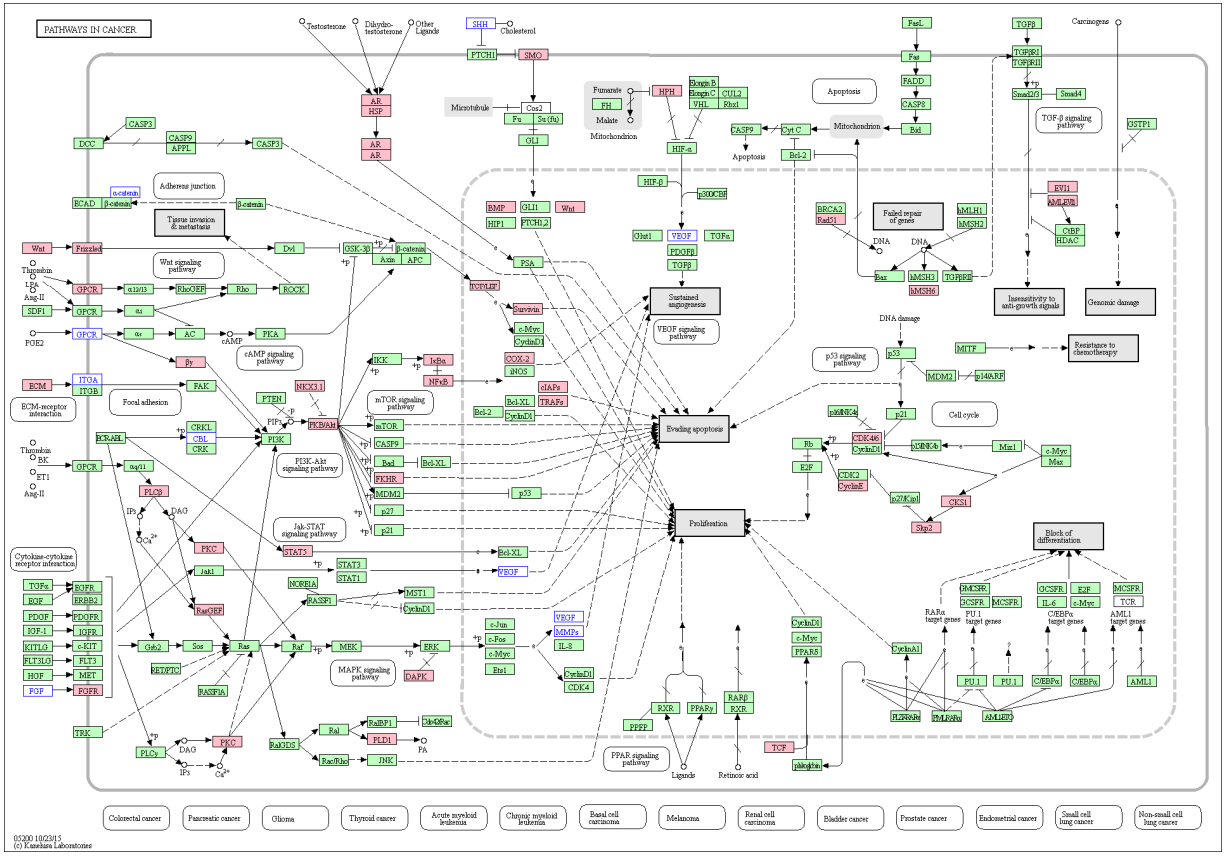

Figure 11. Genes related to cancer were mapped by KEGG pathway analysis. Pink boxes represent upregulated genes, and blue outlined boxes represent downregulated genes in the R1 or R2 groups. Green boxes represent other members in the pathway in *Homo sapiens*.

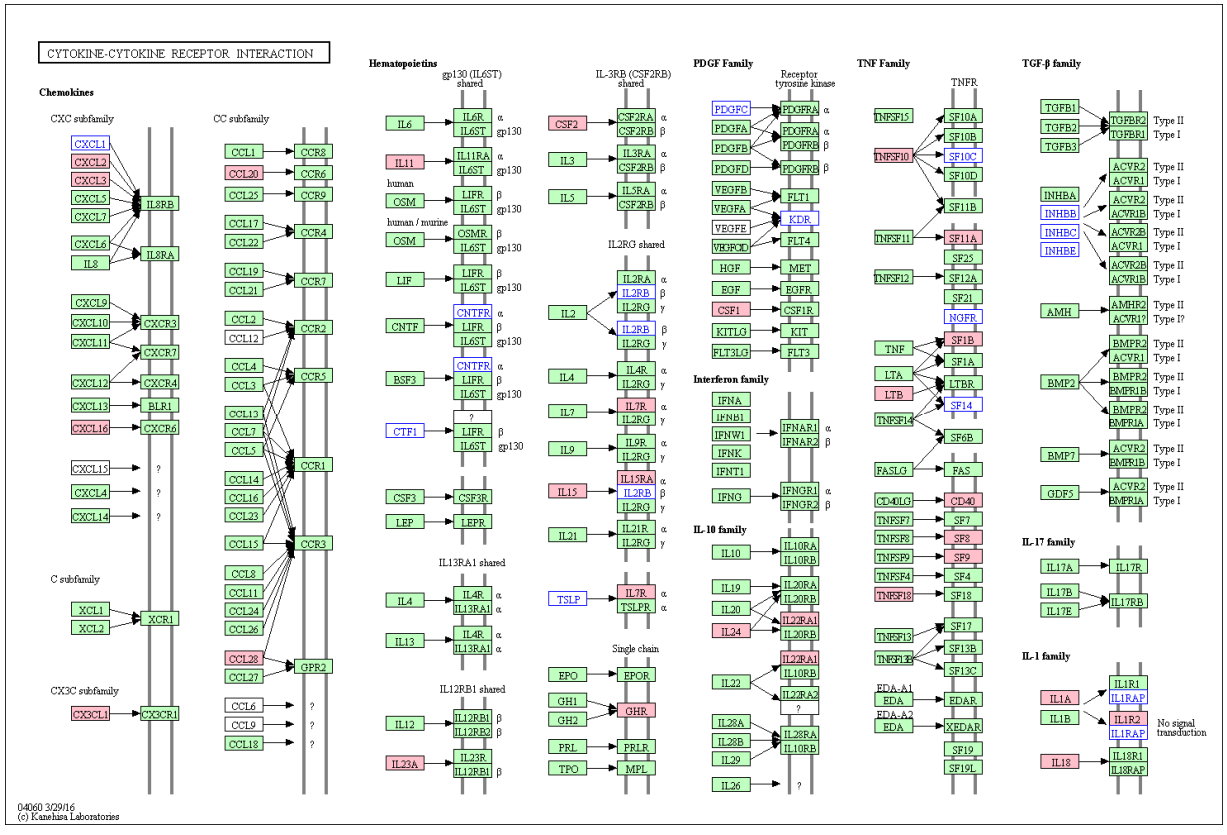

Figure 12. Genes related to cytokine-cytokine receptor interactions were mapped by KEGG pathway analysis. Pink boxes represent upregulated genes, and blue outlined boxes represent downregulated genes in the R1 or R2 groups. Green boxes represent other members in the pathway in *Homo sapiens*.

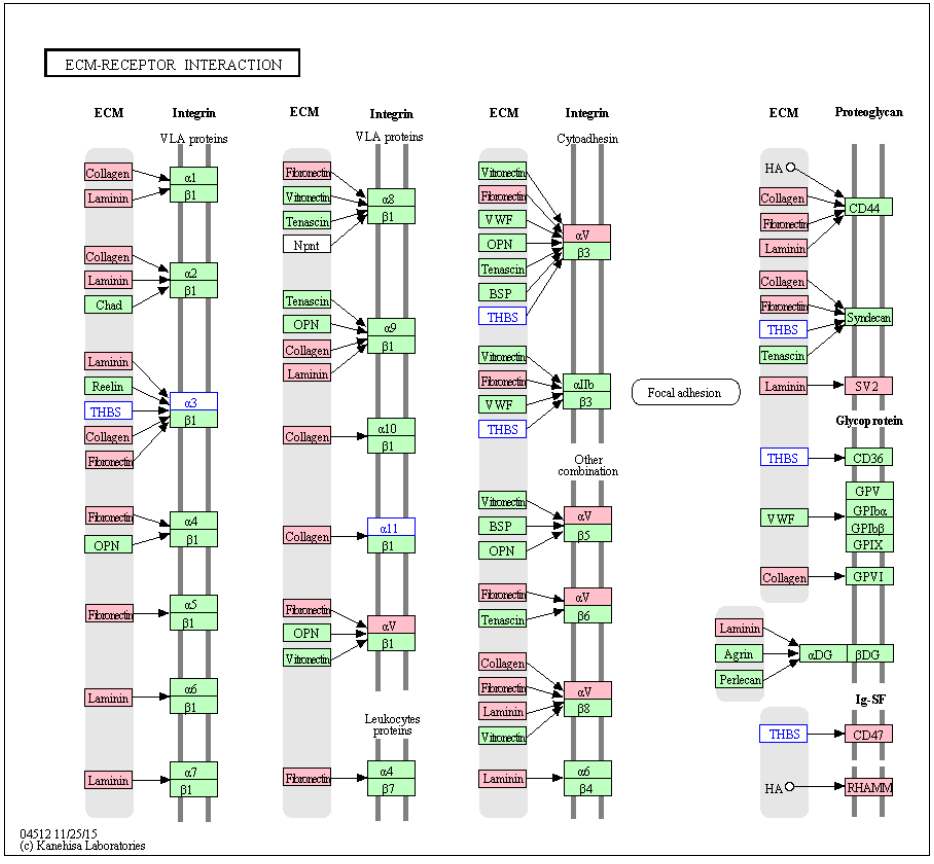

Figure 13. Genes related to extracellular matrix-receptor interactions were mapped by KEGG pathway analysis. Pink boxes represent upregulated genes, and blue outlined boxes represent downregulated genes in the R1 or R2 groups. Green boxes represent other members in the pathway in *Homo sapiens*.

DISCUSSION

To date, the associations or cross-talk between the oncogenic driver pathways in cancer cells and the immunoregulatory pathways, involving such players as PD-L1, have not been fully elucidated.[21] Recently Akbay et al. reported activation of the PD-L1 pathway by activation of the EGFR pathway in EGFR-driven lung tumors, raising the possibility that other oncogenes may drive immune escape.[22] Thereafter, upregulation of the PD-L1 pathway by ALK pathway activation was reported in ALK-positive NSCLC cells.[9] Based on these findings, we conclude that oncogenic driver signaling does not only have antitumor effects through inhibition of the tyrosine kinase pathway itself but also remodels the tumor microenvironment to induce immune tolerance.

In melanoma, several studies demonstrated an increase in PD-L1 expression in BRAF inhibitor-resistant cell lines.[21,23,24] Furthermore, Kakavand et al. found that patient tumors that were positive for PD-L1 at baseline exhibited a significant decrease in PD-L1 expression during progression, whereas patient tumors that were negative for PD-L1 expression at baseline exhibited a significant increase in PD-L1 expression during progression when treated with BRAF inhibitor.[25]

Although obtaining a biopsy of melanoma tumor tissue is easier due to the availability of the cutaneous location, obtaining biopsies from metastatic lung cancer tissues are difficult. Accordingly, reports comparing tumor tissue before and after treatment with chemotherapeutic agents have been rare for lung cancer.

Recently, PD-L1 expression was reported to be markedly increased in a subset of patients with EGFR-mutant NSCLC after gefitinib treatment.[14] In our study, we demonstrated that PD-L1 expression is increased after acquisition of resistance to ALK inhibitor in ALK-positive NSCLC.

PD-L1 expression is induced by the EML4-ALK oncoprotein and attenuated by treatment with the specific ALK inhibitor alectinib or by RNAi with ALK siRNAs in EML4-ALK-positive NSCLC.[9] Our results also showed that PD-L1 expression is increased in ALK inhibitor-resistant NSCLC cells. Thus, we speculated that PD-L1 expression is initially downregulated after ALK inhibitor treatment and thereafter upregulated after establishment of resistance. In melanoma, the inhibition of PD-L1 by dabrafenib, trametinib, and dabrafenib and trametinib was transient *in vitro* and was not associated with the activation status of the pathway over time.[24] In A375 melanoma cells treated with dabrafenib, trametinib, or dabrafenib and trametinib over a 30-d time course, PD-L1 mRNA levels increased steadily to day 30 after an initial reduction that was observed in the first 8 d.[24] We therefore investigated the changes in PD-L1 expression during treatment of NSCLC with ALK inhibitors. In our study, PD-L1 expression increased over time as ALK-positive lung cancer cell lines were exposed to several ALK inhibitors. Although the initial reduction was not prominent, PD-L1 expression appeared not to increase during the initial 50 d of treatment.

In our analysis with TILs, the proportion of $CD68^+$ TILs was significantly decreased in the post-treatment ALK-positive NSCLC, and expression of CD3,

CD8, and PD-1 tended to be lower in the post-treatment group than in the pre-treatment group. Tumor-associated macrophages are reported to play a pro-tumor role,[26] In melanoma, no significant change in CD68-expressing macrophages was observed at any time point (i.e., early during treatment and during progression) in the BRAFi-treated patients, while a significant increase in $CD4^+$, $CD8^+$, and $PD\text{-}1^+$ intratumoral lymphocytes was observed from pre-treatment to early during treatment. Furthermore, there was a significant increase in TILs from pre-treatment to early time points during treatment, and then TILs decreased significantly from early during treatment to times during progression.[25] Taken together, these results indicate that treatment-related changes in the immune system is a highly dynamic process, and our observed results with may be a picture taken in the middle of this dynamic process. And the influence of ALK inhibition and ALK inhibitor resistance on tumor-associated macrophages warrants further investigation.

Our RNA sequencing results revealed that the gene expression profiles differed between the H3122 parental cells and the cell lines from the single- and double-resistant groups. Moreover, the R1 and R2 groups were distinct according to clustering analysis, and the differences (fold changes) tended to be greater in the double-resistant group.

Among the top 20 differentially expressed genes in the R1 or R2 groups compared to the H3122 parental cell line, the majority of the genes were associated with the immune system. OR2W1 exhibited a $\log_2$ fold change of >16 in both groups. GO annotations related to this gene include G-protein-coupled receptor activity and

olfactory receptor activity, while the relationship between this gene and tumors has been reported infrequently.[27] OR2W1 is reportedly upregulated following 48-h asbestos exposure in lung cancer cell lines[28] and has been associated with breast and endometrial cancer cells.[29,30] C1RL-AS1 and RNU6-485P, which were profoundly downregulated in the ALK inhibitor-resistant groups also lacks conclusive evidence for its role in cancer, while Complement C1r subcomponent-like protein (C1RL) is related to immune system processes. Further research is necessary to elucidate the relationships of these genes to ALK inhibitor resistance and cancer in general.

Expression of PGLYRP4, CCL20, DEFB4A, LTB, and CDH6 was altered by >6 absolute $\log_2$ fold in both R1 and R2 groups relative to parental H3122 cells. PGLYRRP4 is related to immune homeostasis and is induced in response to bacterial infection, limiting the innate immune response and preventing excessive inflammation.[31] GO annotations related to CCL20 include cytokine activity and chemokine activity, and several reports demonstrated the relationship between this gene and aggressive tumor behavior,[32,33] tumor-promoting macrophages,[34] regulatory T cells, myeloid-derived suppressor cells,[35] and the epithelial-mesenchymal transition.[36] DEFB4 has been reported to be associated with immune response in NSCLC.[37,38] LTB was reported to act as one of the central mediators in liver cancer formation with chronic liver injury.[39] Recently, utilization of the lymphotoxin β (LTB) pathway was described as a novel strategy to overcome resistance to PD-L1 blockade.[22] Meanwhile, CDH6 was reported to promote the

epithelial-mesenchymal-transition and an aggressive phenotype in several cancers.[40-42]

AB019440.1 and AB019440.50 expression was profoundly decreased in both R1 and R2 groups compared to H3122 cell lines. AB019440.1 encodes immunoglobulin heavy variable 1-18, and immunoglobulin heavy variable genes have been reported to be associated with several hematologic malignancies.[43-46] In addition, CD177, PIGR, ASB2, S100A8, and C2, CFB were related to the immune system.[27,47] S100A8 was found to be increased in PD-L1-upregulated pancreatic cancers[48] and associated with tumor-infiltrating macrophages in several types of cancer cells.[49,50]

Of the several immune checkpoints identified, only PD-L1 gene expression increased as resistance to ALK inhibitors became more profound, suggesting that the role of immune checkpoints other than PD-L1 pathway may be minimal. No alterations in expression of genes of other oncogenic pathways and lung adenocarcinoma-related genes were observed in the ALK inhibitor-resistant cells, indicating a lack of bypass pathway activation in these cell lines.

Biologic processes and pathways involving the differentially expressed genes were analyzed using ToppGene and KEGG mapper. Several pathways related to the immune system, cancer, and extracellular matrix-receptor interactions were identified. Wnt signaling and heat shock protein pathways associated with proliferation and evasion of apoptosis as well as the cell cycle pathway were

involved in the cancer pathway. Several reports have demonstrated the association between ALK inhibitor resistance and heat shock protein[51] and the epithelial-mesenchymal transition.[52] To the best of my knowledge, the Wnt signaling pathway has not been reported in relation to ALK-positive NSCLC; however, a few reports have described the relationship between Wnt signaling and ALK-positive anaplastic large cell lymphoma or resistance to chemotherapy.[53-55] Taken together, these data indicate that resistance to ALK inhibitors in NSCLC is related to the immune system, several cancer pathways, and the epithelial-mesenchymal transition.

The main limitations of this study were its retrospective nature and the small number of patients included. Furthermore, pre- and post-treatment tumor specimens were non-paired. These limitations stem from the facts that ALK-positive NSCLC is a relatively rare disease and that biopsy after disease progression is not a routine practice. Nevertheless, this study is the first report to describe alterations in PD-L1 expression related to resistance to ALK inhibitors in ALK-positive NSCLC patients. Thus, this study is expected to provide the foundation for further investigations of the role of PD-1/PD-L1 pathway in resistance to target agents.

We performed RNA sequencing with parental as well as single- and double-resistant -cell lines to ALK inhibitor. Because of the paucity of the cell lines, statistical significance could not be estimated. Notwithstanding, we found that the direction and the degree of gene expression changes between the single-resistance

and the H3122 parental cells were reproducible by the comparison of the double-resistant cell lines and the H3122 parental cells, suggesting that these data are meaningful. Furthermore, we identified genes related to the immune system as factors that are involved in the process of development of resistance to ALK inhibitors.

In conclusion, PD-L1 expression was consistently increased after acquisition of resistance to ALK inhibitor in tumor specimens from lung cancer patients and in cell lines. Thus, the PD-1/PD-L1 pathway is associated with resistance to ALK inhibitors in ALK-rearranged NSCLC. Future studies will further examine the relationship between the PD/1PD-L1 pathway and ALK inhibitor resistance.

REFERENCES

1. Miller KD, Siegel RL, Lin CC, et al. Cancer treatment and survivorship statistics, 2016. CA Cancer J Clin 2016;66:271-89.
2. Jung KW, Won YJ, Oh CM, et al. Prediction of Cancer Incidence and Mortality in Korea, 2016. Cancer Res Treat 2016;48:451-7.
3. Molina JR, Yang P, Cassivi SD, Schild SE, Adjei AA. Non-small cell lung cancer: epidemiology, risk factors, treatment, and survivorship. Mayo Clin Proc 2008;83:584-94.
4. Soda M, Choi YL, Enomoto M, et al. Identification of the transforming EML4-ALK fusion gene in non-small-cell lung cancer. Nature 2007;448:561-6.
5. Thomas RK. Overcoming drug resistance in ALK-rearranged lung cancer. N Engl J Med 2014;370:1250-1.
6. Katayama R, Friboulet L, Koike S, et al. Two novel ALK mutations mediate acquired resistance to the next-generation ALK inhibitor alectinib. Clinical cancer research : an official journal of the American Association for Cancer Research 2014;20:5686-96.
7. Hanahan D, Weinberg RA. Hallmarks of cancer: the next generation. Cell 2011;144:646-74.
8. Sundar R, Soong R, Cho BC, Brahmer JR, Soo RA. Immunotherapy in the treatment of non-small cell lung cancer. Lung Cancer 2014;85:101-9.
9. Ota K, Azuma K, Kawahara A, et al. Induction of PD-L1 Expression by the EML4-ALK Oncoprotein and Downstream Signaling Pathways in Non-Small Cell Lung Cancer. Clinical cancer research : an official journal of the American Association for Cancer Research 2015;21:4014-21.
10. D'Incecco A, Andreozzi M, Ludovini V, et al. PD-1 and PD-L1 expression in molecularly selected non-small-cell lung cancer patients. Br J Cancer 2015;112:95-102.
11. Brahmer J, Reckamp KL, Baas P, et al. Nivolumab versus Docetaxel in

Advanced Squamous-Cell Non-Small-Cell Lung Cancer. N Engl J Med 2015;373:123-35.

12. Borghaei H, Paz-Ares L, Horn L, et al. Nivolumab versus Docetaxel in Advanced Nonsquamous Non-Small-Cell Lung Cancer. N Engl J Med 2015;373:1627-39.

13. Azuma K, Ota K, Kawahara A, et al. Association of PD-L1 overexpression with activating EGFR mutations in surgically resected nonsmall-cell lung cancer. Ann Oncol 2014;25:1935-40.

14. Han JJ, Kim DW, Koh J, et al. Change in PD-L1 Expression After Acquiring Resistance to Gefitinib in EGFR-Mutant Non-Small-Cell Lung Cancer. Clin Lung Cancer 2016;17:263-70 e2.

15. Koh J, Go H, Keam B, et al. Clinicopathologic analysis of programmed cell death-1 and programmed cell death-ligand 1 and 2 expressions in pulmonary adenocarcinoma: comparison with histology and driver oncogenic alteration status. Mod Pathol 2015;28:1154-66.

16. Kim S, Kim TM, Kim DW, et al. Heterogeneity of genetic changes associated with acquired crizotinib resistance in ALK-rearranged lung cancer. J Thorac Oncol 2013;8:415-22.

17. Kim YT, Kim TY, Lee DS, et al. Molecular changes of epidermal growth factor receptor (EGFR) and KRAS and their impact on the clinical outcomes in surgically resected adenocarcinoma of the lung. Lung Cancer 2008;59:111-8.

18. Trapnell C, Roberts A, Goff L, et al. Differential gene and transcript expression analysis of RNA-seq experiments with TopHat and Cufflinks. Nature protocols 2012;7:562-78.

19. Chen J, Bardes EE, Aronow BJ, Jegga AG. ToppGene Suite for gene list enrichment analysis and candidate gene prioritization. Nucleic acids research 2009;37:W305-W11.

20. Kanehisa M, Goto S, Sato Y, Furumichi M, Tanabe M. KEGG for integration and interpretation of large-scale molecular data sets. Nucleic acids research 2011:gkr988.

21. Atefi M, Avramis E, Lassen A, et al. Effects of MAPK and PI3K pathways on PD-L1 expression in melanoma. Clinical cancer research : an official journal of the American Association for Cancer Research 2014;20:3446-57.
22. Akbay EA, Koyama S, Carretero J, et al. Activation of the PD-1 pathway contributes to immune escape in EGFR-driven lung tumors. Cancer discovery 2013;3:1355-63.
23. Jiang X, Zhou J, Giobbie-Hurder A, Wargo J, Hodi FS. The activation of MAPK in melanoma cells resistant to BRAF inhibition promotes PD-L1 expression that is reversible by MEK and PI3K inhibition. Clinical cancer research : an official journal of the American Association for Cancer Research 2013;19:598-609.
24. Liu L, Mayes PA, Eastman S, et al. The BRAF and MEK Inhibitors Dabrafenib and Trametinib: Effects on Immune Function and in Combination with Immunomodulatory Antibodies Targeting PD-1, PD-L1, and CTLA-4. Clinical cancer research : an official journal of the American Association for Cancer Research 2015;21:1639-51.
25. Kakavand H, Wilmott JS, Menzies AM, et al. PD-L1 Expression and Tumor-Infiltrating Lymphocytes Define Different Subsets of MAPK Inhibitor-Treated Melanoma Patients. Clinical cancer research : an official journal of the American Association for Cancer Research 2015;21:3140-8.
26. Noy R, Pollard JW. Tumor-associated macrophages: from mechanisms to therapy. Immunity 2014;41:49-61.
27. Gene Ontology Consortium: going forward. Nucleic acids research 2015;43:D1049-56.
28. Nymark P, Lindholm PM, Korpela MV, et al. Gene expression profiles in asbestos-exposed epithelial and mesothelial lung cell lines. BMC genomics 2007;8:62.
29. Rafique S, Thomas JS, Sproul D, Bickmore WA. Estrogen-induced chromatin decondensation and nuclear re-organization linked to regional epigenetic regulation in breast cancer. Genome biology 2015;16:145.
30. Ren CE, Zhu X, Li J, et al. Microarray analysis on gene regulation by

estrogen, progesterone and tamoxifen in human endometrial stromal cells. International journal of molecular sciences 2015;16:5864-85.

31. Guo L, Karpac J, Tran SL, Jasper H. PGRP-SC2 promotes gut immune homeostasis to limit commensal dysbiosis and extend lifespan. Cell 2014;156:109-22.

32. Yamamura K, Baba Y, Nakagawa S, et al. Human Microbiome Fusobacterium Nucleatum in Esophageal Cancer Tissue Is Associated with Prognosis. Clinical cancer research : an official journal of the American Association for Cancer Research 2016.

33. Ignacio RM, Kabir SM, Lee ES, Adunyah SE, Son DS. NF-kappaB-Mediated CCL20 Reigns Dominantly in CXCR2-Driven Ovarian Cancer Progression. PloS one 2016;11:e0164189.

34. Nandi B, Shapiro M, Samur MK, et al. Stromal CCR6 drives tumor growth in a murine transplantable colon cancer through recruitment of tumor-promoting macrophages. Oncoimmunology 2016;5:e1189052.

35. Chang AL, Miska J, Wainwright DA, et al. CCL2 Produced by the Glioma Microenvironment Is Essential for the Recruitment of Regulatory T Cells and Myeloid-Derived Suppressor Cells. Cancer research 2016;76:5671-82.

36. Liu Y, Wang J, Ni T, Wang L, Wang Y, Sun X. CCL20 mediates RANK/RANKL-induced epithelial-mesenchymal transition in endometrial cancer cells. Oncotarget 2016;7:25328-39.

37. Li J, Bi L, Shi Z, et al. RNA-Seq analysis of non-small cell lung cancer in female never-smokers reveals candidate cancer-associated long non-coding RNAs. Pathology, research and practice 2016;212:549-54.

38. Al Zeyadi M, Dimova I, Ranchich V, et al. Whole genome microarray analysis in non-small cell lung cancer. Biotechnology, biotechnological equipment 2015;29:111-8.

39. Endig J, Buitrago-Molina LE, Marhenke S, et al. Dual Role of the Adaptive Immune System in Liver Injury and Hepatocellular Carcinoma Development. Cancer cell 2016;30:308-23.

40. Gugnoni M, Sancisi V, Gandolfi G, et al. Cadherin-6 promotes EMT and cancer metastasis by restraining autophagy. Oncogene 2016.
41. Sancisi V, Gandolfi G, Ragazzi M, et al. Cadherin 6 is a new RUNX2 target in TGF-beta signalling pathway. PloS one 2013;8:e75489.
42. Xu L, Wang Z, Li XF, et al. Screening and identification of significant genes related to tumor metastasis and PSMA in prostate cancer using microarray analysis. Oncology reports 2013;30:1920-8.
43. Baliakas P, Agathangelidis A, Hadzidimitriou A, et al. Not all IGHV3-21 chronic lymphocytic leukemias are equal: prognostic considerations. Blood 2015;125:856-9.
44. Xochelli A, Agathangelidis A, Kavakiotis I, et al. Immunoglobulin heavy variable (IGHV) genes and alleles: new entities, new names and implications for research and prognostication in chronic lymphocytic leukaemia. Immunogenetics 2015;67:61-6.
45. Bikos V, Darzentas N, Hadzidimitriou A, et al. Over 30% of patients with splenic marginal zone lymphoma express the same immunoglobulin heavy variable gene: ontogenetic implications. Leukemia 2012;26:1638-46.
46. Tobin G, Thunberg U, Karlsson K, et al. Subsets with restricted immunoglobulin gene rearrangement features indicate a role for antigen selection in the development of chronic lymphocytic leukemia. Blood 2004;104:2879-85.
47. Nishiyama T, Kuroda S, Takiguchi E, et al. The ASB2beta Ubiquitin-interacting motif is involved in its monoubiquitination. Biochemical and biophysical research communications 2012;420:487-91.
48. Birnbaum DJ, Finetti P, Lopresti A, et al. Prognostic value of PDL1 expression in pancreatic cancer. Oncotarget 2016.
49. Zha H, Sun H, Li X, et al. S100A8 facilitates the migration of colorectal cancer cells through regulating macrophages in the inflammatory microenvironment. Oncology reports 2016;36:279-90.
50. Lim SY, Yuzhalin AE, Gordon-Weeks AN, Muschel RJ. Tumor-infiltrating monocytes/macrophages promote tumor invasion and migration by upregulating

S100A8 and S100A9 expression in cancer cells. Oncogene 2016.
51. Sang J, Acquaviva J, Friedland JC, et al. Targeted inhibition of the molecular chaperone Hsp90 overcomes ALK inhibitor resistance in non-small cell lung cancer. Cancer discovery 2013;3:430-43.
52. Kim HR, Kim WS, Choi YJ, Choi CM, Rho JK, Lee JC. Epithelial-mesenchymal transition leads to crizotinib resistance in H2228 lung cancer cells with EML4-ALK translocation. Molecular oncology 2013;7:1093-102.
53. Wu C, Zhang HF, Gupta N, et al. A positive feedback loop involving the Wnt/beta-catenin/MYC/Sox2 axis defines a highly tumorigenic cell subpopulation in ALK-positive anaplastic large cell lymphoma. Journal of hematology & oncology 2016;9:120.
54. Armanious H, Gelebart P, Anand M, Lai R. Identification of a novel crosstalk between casein kinase 2alpha and NPM-ALK in ALK-positive anaplastic large cell lymphoma. Cellular signalling 2013;25:381-8.
55. Chikazawa N, Tanaka H, Tasaka T, et al. Inhibition of Wnt signaling pathway decreases chemotherapy-resistant side-population colon cancer cells. Anticancer research 2010;30:2041-8.

국문 초록

배경 및 목적: ALK (anaplastic lymphoma kinase, 역형성 림프종 인산화효소) 억제제는 ALK 양성 비소세포폐암 환자에서 표준 치료이나 대부분의 환자가 시간이 지남에 따라 내성을 획득하게 된다. PD-L1 (Programmed cell death-ligand 1)은 암 세포에 발현하여 면역 회피를 일으키며 암의 진행을 촉진한다. PD-1 (programmed cell death-1)/PD-L1 발현과 ALK 양성 비소세포폐암에서 ALK 억제제 내성획득의 연관성에 대해서는 거의 밝혀져 있지 않다. 이에 연구자는 ALK 양성 비소세포폐암 조직과 세포주에서 ALK 억제제 내성 획득에 따른 PD-L1 발현의 변화에 대해 평가하였다.

방법: 총 26명의 전이성 ALK 양성 비소세포폐암 환자의 암 조직이 분석되었으며, 그 중 11 명은 ALK 억제제를 사용하기 전, 나머지 15 명은 ALK 억제제 내성을 얻은 후의 환자였다. 면역조직염색으로 ALK 억제제 내성 획득 전후의 암 조직에서 PD-L1과 림프구 표지자의 차이를 분석하였다. PD-L1 H-score는 염색강도 수치(0, 1, 2, 3)와 비율의 곱으로 계산하였으며, PD-L1 양성은 강도 수치와 10%를 기준으로 구분하여 분석하였다.

또한 ALK 유전자 전위를 가지는 폐암 세포주인 H3122에 ALK 억제제를 노출시켜 ALK 억제제 내성 세포주인 H3122CR1, LR1, CH1을 수립

하였다. 그리고 나서 크리조티닙 내성 세포주인 H3122CR1에 2세대 ALK 억제제들을 노출시켜 2차 내성 세포주인 H3122CR1LR1, CR1CH1을 만들었다. Western blotting과 유세포검사 및 정량적 중합효소연쇄반응을 이용하여 PD-L1 발현의 변화를 비교하였다. 또한 RNA 시퀀싱을 이용하여 H3122, CR1, LR1, CH1, CR1LR1, CR1CH1 세포주에서의 유전자 발현을 조사하였으며, 1차 내성 세포주와 2차 내성 세포주를 그룹화하여 H3122 모세포주와 각각 비교분석하였다. 또한 차별발현 유전자를 이용하여 생물학적 과정과 경로를 분석하였다.

결과: PD-L1 H-score의 평균값은 ALK 억제제 치료 전 환자 암 조직에서 6.5, 치료 후 내성 발생 후 35.0으로 5.42배의 차이를 보였다(p = 0.163). 또한 치료 후 환자에서 치료 전 환자에 비해 PD-L1 양성의 비율이 더 높았다(3명(20.0%) 대 0명(0.0%), p = 0.175). 제곱 밀리미터당 CD68의 평균 개수는 치료 전에 181.6±115.4, 치료 후에 90.8±48.9 이었다(p = 0.030). 체외 실험에서도, ALK 억제제 치료를 받지 않은 모세포주인 H3122에 비해 ALK 억제제 내성을 갖는 세포주들에서 PD-L1이 높게 발현되었다. 1차 내성 세포주들에 비해 2차 내성 세포주들에서 PD-L1의 발현이 높았다. 이런 경향은 전체 단백질, 표면 단백질, mRNA 수준에서 동일하게 관찰되었다. RNA 시퀀싱 결과, 모세포주에 비해 1차 내성 세포주 및 2차 내성 세포주에서 PGLYRRP4, CCL20, DEFB4A, LTB, and CDH6 등 면역 관련 유전자들의 발현 변

화가 뚜렷하였다. 또한 ALK 억제제 내성이 심해질수록 PD-L1 발현은 증가하였다. 그리고 차별발현 유전자를 이용한 생물학적 과정 및 경로분석 에서는 사이토카인 경로 등 면역관련 경로가 ALK 억제제 내성에 유의하게 관여되어 있었다.

결론: ALK 양성 비소세포폐암 조직과 세포주에서 ALK 억제제에 대한 내성을 획득한 후에 PD-L1 발현은 증가되었다. 다른 ALK 억제제에 대한 내성이 추가될수록 PD-L1 발현은 더 증가하였다. 이에 ALK 억제제 내성 획득과 PD-1/PD-L1 발현양상의 연관성에 대하여 추가적인 연구가 필요하다.

주요어: 역형성 림프종 인산화효소(ALK), 폐암, ALK 억제제, 내성, PD-L1, 면역관문
학 번: 2011-31138